

Article

# Physical and Electrochemical Performances of Cold Sprayed Pb Electrodes

Guosheng Huang <sup>1,\*</sup>, Yaowei Zhuang <sup>1,2</sup> and Wei Fu <sup>3</sup>

<sup>1</sup> Science and Technology on Marine Corrosion and Protection Laboratory, Luoyang Ship Material Research Institute, Qingdao 266237, China; goshen1977@126.com

<sup>2</sup> Qingdao No. 9 High School (Qingdao Foreign Language School), Qingdao 266000, China

<sup>3</sup> State Key Laboratory of Advanced Technology for Materials Synthesis and Processing, Wuhan University of Technology, Wuhan 430070, China; fw82764742@whut.edu.cn

\* Correspondence: huanggs@sunrui.net; Tel.: +86-532-6872-5121

Received: 16 February 2019; Accepted: 4 March 2019; Published: 6 March 2019



**Abstract:** Titanium-based PbO<sub>2</sub> electrodes are widely used for chemical industries, such as electro dialysis, electrolysis, and electrodeposition, to improve the mechanical and life cycle properties of Pb metal electrodes. However, PbO<sub>2</sub> electrodes are usually electrodeposited onto rigid metals due to its soft characteristic, which results in severe passivation problems requiring thin thickness and high porosity. It is of great importance to develop a rigid Pb metal electrode system since thermal spraying and welding methods fail to manufacture such a promising electrode. In the present work, the cold spraying method was used to deposit a pure Pb metal coating with thickness of above 500 μm on Q235 steel substrate. The coating has good physical performances, the porosity is less than 1%, and the bonding strength ranges from 6.25 to 7.75 MPa. The cross-sectional morphology suggests that no through-thickness pores exist in the coating. The oxygen evolution potential is larger than 1.5 V vs. SCE, which is similar to the potential of the titanium-based PbO<sub>2</sub> electrode. Dynamic polarization curves and cyclic voltammetry curves of coated sample in sodium sulfate solution indicate that cold sprayed Pb coating is a good electrode for electrochemical reduction reactions. All our results mean that cold spraying is capable of manufacturing electrode materials for electrochemical industries.

**Keywords:** Pb; cold spray; electrode; roughness; bonding strength; deformation

## 1. Introduction

PbO<sub>2</sub> electrodes are widely used for chemical industries, such as electro dialysis, electrolysis, and electrodeposition, and especially in the production of 1,4-dicyanobutane, which is usually in plate shape (Figure 1 shows a typical schematic setup of a bipolar electrolysis system [1–3]). The distance (*L*) between electrodes in an electrochemical system is always very narrow—always narrower than 3 mm—to improve the reaction efficiency by increasing the turbulence of the electrolyte flow. Any deformations within the welding process and spraying process will lead to electrical connection and short circuit between two neighboring electrodes, which makes the distance larger and decreases the reaction efficiency. Early PbO<sub>2</sub> electrodes were prepared on Pb metal directly by anodic oxidation [4]. However, these kinds of electrodes suffer from poor mechanical properties. Thus, PbO<sub>2</sub> electrodes are usually prepared on some rigid valve metal, such as titanium, tantalum, and zirconium, which have both high mechanical strength and good conductivity. By now, titanium is one of the most widely used substrates for PbO<sub>2</sub> electrodes because titanium has a similar thermal expansion rate as PbO<sub>2</sub> while experiencing temperature changes and good conductivity. Titanium-based PbO<sub>2</sub> anodes fail because of corrosion of the substrate, resulting in an abrupt increase of the cell voltage of the electrochemical system [5,6]. A transition layer was usually used to promote the anticorrosion

performance of titanium-based  $\text{PbO}_2$  electrodes, such as Sn–Sb alloy, tantalum, and Pt. These methods made the electrode manufacturing process more complicated and expensive [7]. To coat Pb on a rigid metal and to oxidize the surface of Pb or  $\text{PbO}$  coating to  $\text{PbO}_2$  is an alternative way to solve this problem. Thermal sprayed Pb coating was tried [8], but the high porosity resulted in the coating having low anticorrosion performance and high electrical resistance. Thus, it is necessary to develop new methods for preparing high density Pb coatings.

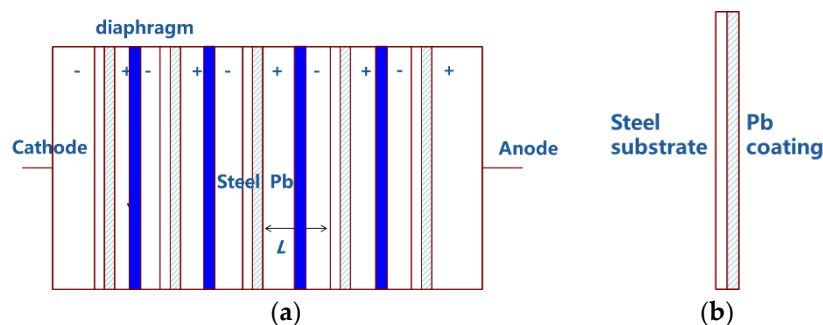


**Figure 1.** (a) Schematic of a bipolar electrolysis system; (b) coating bipolar component.

Cold spray technology is a promising method for preparing dense coatings and electrode components [9,10], and the low heat input leads to minor or no deformation of the substrate. The thickness of the cold sprayed Pb coating can be controlled from 50  $\mu\text{m}$  to several centimeters, which is very suitable for such a bipolar electrode. Regarding cold spraying, in a wind-tunnel experiment, Alkhimov et al. [11,12] found that a metal particle can be deposited onto a substrate when the particle exceeds a certain velocity termed the critical velocity below melting temperature. It was found that cold spraying is a bulk solid coating deposition process [13,14], which is totally different from conventional thermal spray methods. Cold spraying is suitable for preparing dense coatings of up to 100% due to the high kinetic energy of the accelerated particles. Many works previously supported this theoretical possibility and made full dense titanium, aluminum, and copper coatings. However, some researchers also point out that a grade coating structure exists from the surface to the interface. The low processing temperature used results in the coating having a low degree of oxidation during deposition. No phase change occurs in the raw material during cold spraying. Some works have been done on anticorrosion tantalum electrodes used in  $\text{H}_2\text{SO}_4$  solution, which are much more compact than PVD-prepared coatings [15]. Some studies have also focused on Pb electrode coating by thermal spraying, but the coating is obviously inferior to cold sprayed coatings in regard to physical performance.

In the present work, the cold spraying method was used to deposit a smooth Pb coating on Q235 steel substrate as an anode. The physical properties were characterized by energy-dispersive X-ray spectroscopy (EDS), scanning electron microscopy (SEM), and some other methods. The electrochemical performances were evaluated by potentiodynamic polarization curve, cyclic voltammetry, and accelerating electrolysis test.

## 2. Materials and Methods

### 2.1. Raw Powders Used for Coating

The Pb powder manufactured by Hebei Zhuhang Powder company has the following nominal components: Pb,  $\text{PbO}_2$ . The nominal composition of  $\text{PbO}_2$  is about 64.24 wt % according to the provider. The powder's morphology was observed under SEM (XL-30 Scanning Electronic Microscope, manufactured by Philips, Armstrong, The Netherlands) and shown in Figure 2a. It can be seen from Figure 2a that the Pb powder has an irregular shape with the size distribution ranging from 15 to 45  $\mu\text{m}$ . The surface is rather smooth in its raw state. Figure 2b gives the elemental composition of the

powders, the Pb content is about 55.67 at %, which will be used to compare the variation in the coating after cold spraying. It can be seen that the powders include Pb, PbO, and PbO<sub>2</sub>.

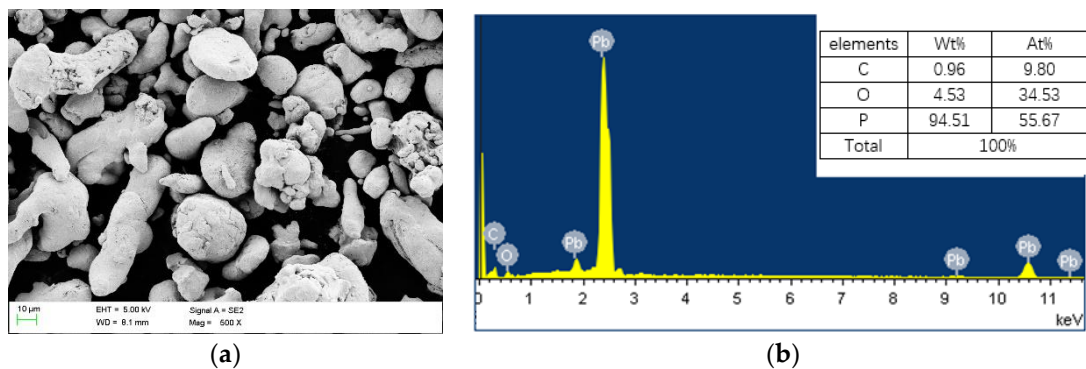


**Figure 2.** Characteristics of raw spraying Pb powders used for preparing Pb coating: (a) morphology of Pb powders; (b) energy-dispersive X-ray spectroscopy (EDS) of Pb powders.

## 2.2. Cold Spraying and Parameters

Type Q235 steel substrate with thickness of 3 mm was sand blasted at room temperature under 0.6 MPa before spraying, which has the following nominal compositions (wt %): C 0.17; Cu 0.08; Mg 0.045; Zn 0.21; Mn 0.60; Ti 0.13; Cr 0.15; P 0.025; Si 0.40 and Fe as balance. A cold spray system (CS-6000 the IMR, Chinese Academy of Sciences, Shenyang, China) was used to deposit Pb coatings. All samples were prepared with the same nozzle geometrical structure (as listed in Table 1) [16]. The thickness of the coatings was estimated to be 500 to 1000  $\mu\text{m}$  after 1 transverse spray. In case of blockage of the nozzle and oxidation, the temperature was set at 298, 348, 398 K, which was relatively low but high enough to get high quality Pb coating. The corresponding coatings were labelled as Pb-1, Pb-2, and Pb-3, respectively. The carrier gas used for accelerating the powder was compressed air. The overlap was about 6 mm per transverse. Correspondingly, three kinds of samples were prepared for investigating the Pb coating and its electrochemical characteristics. It is worth noting that the icing phenomenon was found on the nozzle during spraying at temperatures of 298 and 348 K. The large expansion of gas decreases the temperature below zero and takes away a larger amount heat from the nozzle. This makes the process a real cold process. The temperature was controlled to be relatively low to avoid blocking the nozzle because the Pb powder is soft and can easily block the nozzle's throat at high temperatures. The melting point of Pb metal is about 600 K.

**Table 1.** Nozzle structure summary and spraying parameters used for the CS-6000 cold spray system in the present work.

Parameters	Value
Expansion ratio	2.50
Dimension of nozzle throat	2 mm $\times$ 4 mm
Length of converging part	10 mm
Length of diverging part	100 mm
Dimension of exit	2 mm $\times$ 10 mm
Standoff distant from nozzle exit to substrate	25.0 mm
Carrier gas	Compressed air
Pressure in prechamber	1.6 MPa
Temperature in prechamber	298, 348, 398 K
Powder feeding rate	1.50 g/s
Spraying angle	90° (Perpendicular)
Transverse speed of nozzle	20 mm/s

### 2.3. Characters of Cold Sprayed Pb Coating

#### 2.3.1. Imaging

The samples for SEM (XL-30 Scanning Electronic Microscope, manufactured by Philips, the Netherlands) observation were cut through the cross-section with size 10 mm × 10 mm, abraded with emery paper to #2000 in water, etched in an etching solution (Vol: ice vinegar: water: hydrogen peroxide = 5:4:1) for 60 s, then washed with distilled water and acetone. Microstructural characteristics of cross-section surfaces were observed with SEM (Philips, the Netherlands). All three kinds of samples were examined to evaluate the microstructure of the samples and EDS was used to get the composition of the coating.

#### 2.3.2. Bonding Strength

The pull-off bonding strength test was carried out on a stretcher (DWD-20 computer-controlled tester, manufactured by Yuanming company, Shanghai, China) according to the Pull-off-Strength-Test-Method standard (ASTM-D-4541-02) [17]. The specimen for bonding measurement were disks with the size of  $\Phi$  25 mm × 3 mm. The test specimen was bonded to the fixture by an E-7 Glue, the stretching rate was characterized by the force increasement no higher than  $1000 \pm 100$  N/s in constant. The force ( $F$ , N) was recorded to calculate the bonding strength as the coating broken from the substrate. Then, the bonding strength can be calculated by Equation (1) if the coating was broken at the interface between coating and substrate. Otherwise, the morphology of the broken surface was recorded. The broken surface was observed under SEM to investigate the bonding status and mechanism.

$$BS = F/A \quad (1)$$

where  $BS$  is the bonding strength of samples and  $A$  is the area of the disks.

### 2.4. Electrochemical Behaviour

#### 2.4.1. Potentiodynamic Polarization Test

The cold sprayed Pb coating samples were cut into size of 20 mm × 20 mm, electrically connected to copper leads, and sealed with epoxy resin with a 10 mm × 10 mm area left as the working face. Electrochemical experiments were carried out on a Workstation (Par 2273, Ametek Company, Princeton, NJ, USA) in 5% Na<sub>2</sub>SO<sub>4</sub> solution in a traditional three-electrode system. The pH of the solution was adjusted to about 2 with H<sub>2</sub>SO<sub>4</sub>. The temperature is under room temperature (273.15 K) and the solution was stirred with a magnetic stirrer at a speed of 40 rpm. The sweep speed of potential for potentiodynamic polarization test is 0.167 mV/s. Before the experiments, the potentials of coating samples were measured until the potential variation exceeded no more than  $\pm 3$  mV in 5 min. Potentiodynamic polarization testing was used to determine oxygen evolution potential. The abrupt current rise as the potential increases indicates the evolution of oxygen.

#### 2.4.2. Cyclic Voltammetry

Cyclic voltammetry (CV) is a type of potentiodynamic electrochemical measurement method. In a cyclic voltammetry experiment, the working electrode potential is ramped linearly versus time like linear sweep voltammetry. Cyclic voltammetry takes the experiment a step further than linear sweep voltammetry which ends when it reaches a set potential. When cyclic voltammetry reaches a set potential, the working electrode's potential ramp is inverted. This inversion can happen multiple times during a single experiment. The current at the working electrode is plotted versus the applied voltage to give the cyclic voltammogram trace. The CV experiments were carried out in a three-electrode system in a Na<sub>2</sub>SO<sub>4</sub> solution as demonstrated in potentiodynamic polarization testing. The potential range was selected by pretests, which ranged from hydrogen embrittlement potential to oxygen

evolution potential. The scanning speeds included 10, 20, and 50 mV/s and 100 cycles were repeated for a single electrode at each scanning rate.

#### 2.4.3. Accelerating Electrolysis Test

The accelerating electrolysis test was carried out with a bipolar cell system in a 5 L glass beaker. The working electrodes include the cold sprayed Pb samples, with the size of 20 mm × 25 mm. The counter electrode was pure Pb with a 200 cm<sup>2</sup>. A constant current source (DJS-92, Shanghai Leici Instrument Company, Shanghai, China) was used to provide current for electrolysis. Both the samples were examined in the supporting electrolyte. The supporting electrolyte was 1 mol/L H<sub>2</sub>SO<sub>4</sub> solution. The temperature was controlled at 315 K in a thermostatic water bath. The current density was set as 1 A/cm<sup>2</sup>. The cell voltages of all accelerating electrolysis tests were measured during the test until the cell voltage rises abruptly to higher than 10 V, then the experiment was halted. After that, the weight losses of the electrode samples were calculated. The surface morphology of the samples after testing were observed with SEM and XRD to investigate the failure type and mechanism.

### 3. Results

#### 3.1. Characteristics of Coating Thickness around the Holes

Figure 3 shows the macromorphology of cold sprayed Pb coating on Q235 Steel at different temperatures. It can be seen that a dense bonding layer was formed on the substrate at each temperature. The Pb metal is very soft and can be deposited onto substrate under room temperature of 298 K. Due to the unstable powder feeding rate, the coating surface has many sharp mountain-shaped deposits [18]. Figure 4 shows the surface micromorphology of cold sprayed Pb coating at different temperatures. The morphologies of the coatings are all compact. No pores can be found on the surface of the coatings. There are many crashed particles on the coating surfaces, which have the shape of thermal sprayed particles. The EDS analysis of the coatings and their corresponding element content are shown in Figure 4. Although the temperature is very low (below 398 K), oxidation occurs during the cold spraying process. The oxidation degree increases as the temperature increases. When the temperature is 398 K, the elemental oxygen content reaches about 44.72 at %. Compared to the raw powder, the oxygen content increases by about 10 percent during coating. Pb is sensitive to oxygen and exposure to the atmosphere can lead to oxidation. No raw powder can be found on the surface of each coating, which suggests that the particles deform severely. No raw powder shape can be retained during the impaction for such soft metal. For general metal materials, the up-semi particles hardly deform since their hardness is too high to influence the up-semi part so that raw powder shape particles can be found on the surface of most other metals. Figure 5 shows the cross-sectional micromorphology of cold sprayed Pb coatings at different temperatures. The fracture morphologies of the coatings indicate that a typical ductile dimple fracture pattern occurred on each coating. The three coating samples were all separated with a clamp directly without polishing. It has been considered that the cold sprayed coating has no ductility after experiencing large deformation. Larger deformation leads to the yielding of materials and the elasticity of the materials disappears, which results in the material's low tensile strength. Post heat treatment is necessary to recover the elastic property of cold sprayed building deposits. However, Pb is different from other metals. Its soft character makes the deformation easier and melting occurs more easily. The polished cross-sectional morphologies are shown at the right side for each coating samples. All samples have a very dense appearance (upper part is Pb coatings, some abrasive particles can be found on some parts of the samples), which verifies the severe deformation of particles. The porosity is lower than 1% for all samples according to Imaging treatment software ImageJ (National Institutes of Health, Bethesda, MD, USA, standard grit method).

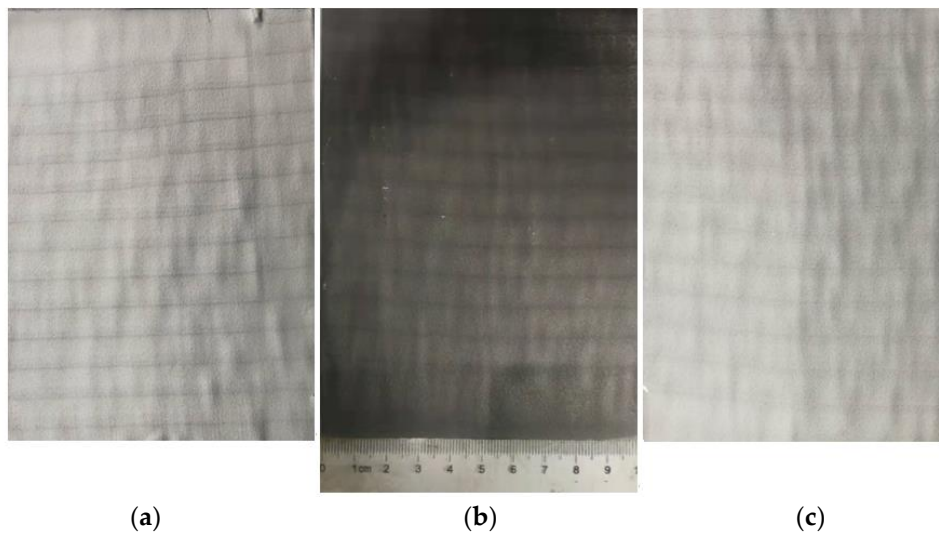


**Figure 3.** Macromorphology of cold sprayed Pb coatings on Q235 Steel: (a) 298 K, 1.6 MPa; (b) 348 K, 1.6 MPa; (c) 398 K, 1.6 MPa.

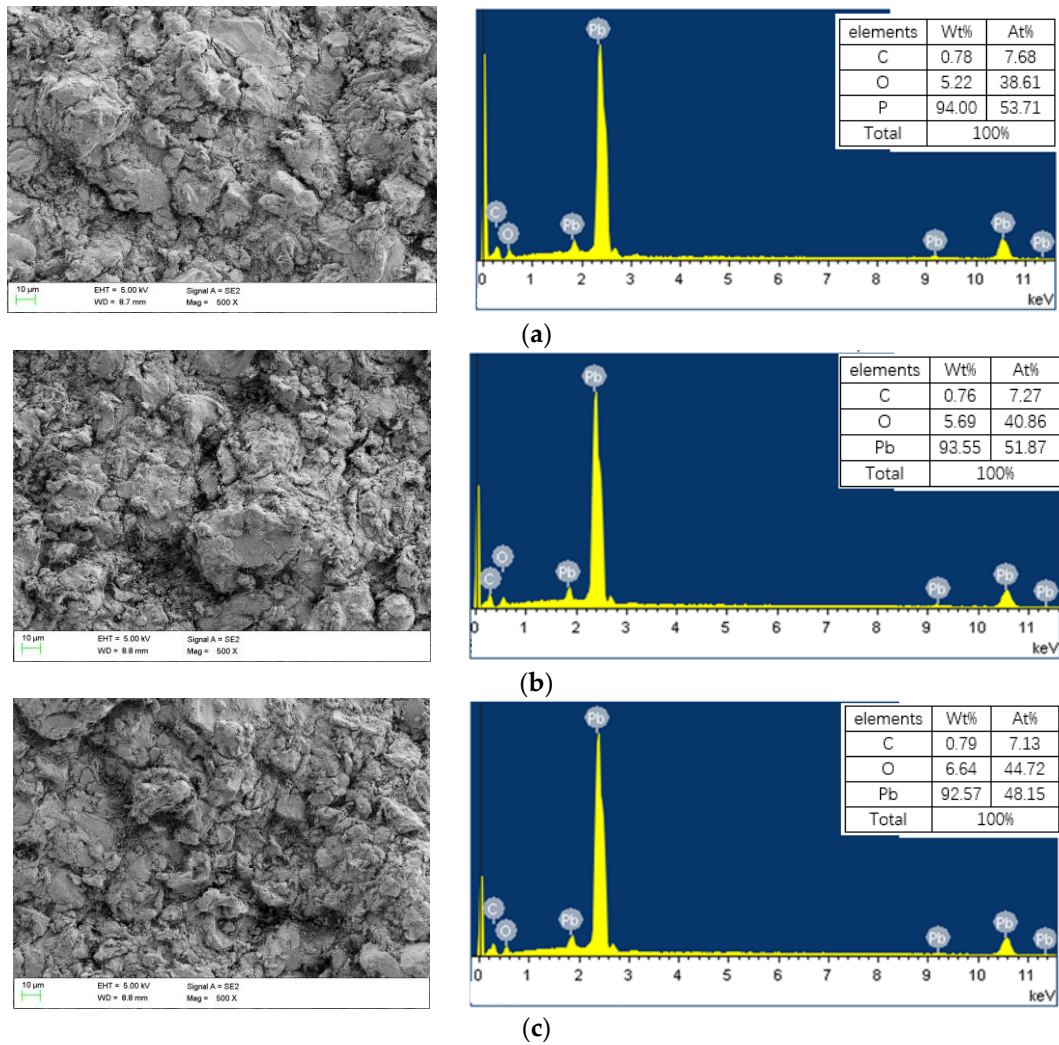


**Figure 4.** Surface micromorphology of cold sprayed Pb coatings on Q235 Steel: (a) 298 K, 1.6 MPa; (b) 348 K, 1.6 MPa; (c) 398 K, 1.6 MPa.

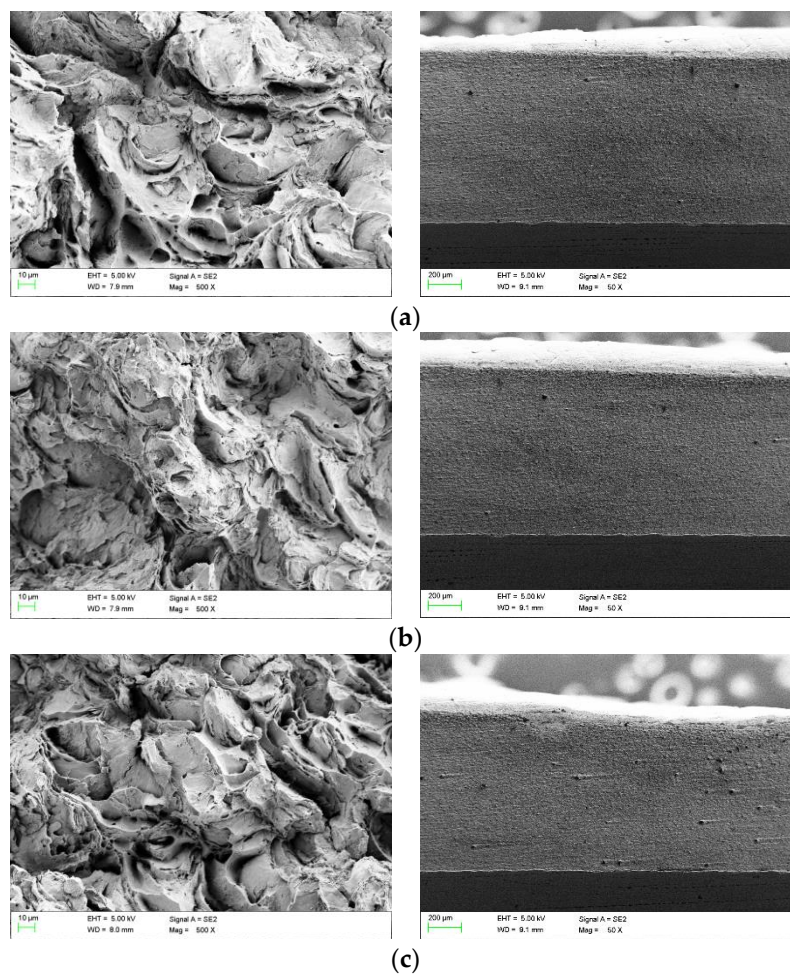


**Figure 5.** Cross-sectional micromorphology and its EDS analysis of cold sprayed Pb coatings on Q235 Steel: (a) 298 K, 1.6 MPa; (b) 348 K, 1.6 MPa; (c) 398 K, 1.6 MPa.

### 3.2. Pull-off Bonding Strength of Pb Coating on Steel Substrate

The bonding strength of three kinds of samples are listed in Table 2, which range from 6.25 to 7.75 MPa. The fracturing of all samples occurred at the interface between coating and substrate, but there are also some inner fractures since much Pb was left on the iron substrate. The fracture morphologies of the coatings indicate that the typical ductile dimple fracture pattern occurred on each coating at the interface, which is the same with the cross-sectional surface. Sample Pb-1 ranges from 6.25 to 7.42 MPa, sample Pb-2 ranges from 6.71 to 7.75 MPa, and sample Pb-3 ranges from 6.52 to 7.35 MPa. It can be seen that the bonding strengths of different spraying parameters differ very little among three samples. There is little correlation between bonding strengths and spraying temperatures. The surface preparation conditions for the three samples were identical and the powders used in the spraying were the same. This phenomenon is mainly because the bonding strength is only determined by the roughness of the substrate. Usually, cold sprayed coatings can be controlled by spraying temperature because elevated temperature can accelerate particles to higher velocities and soften the particles, resulting in larger deformation. However, the Pb particles are so soft that there is no need to accelerate the particles to a very high velocity. Complete deformation can be realized at very low velocity. Soft Pb particles usually create no craters on Q235 steel, which is different from other metals. If the particles can create craters on the surface of the substrate, the bonding strength will be determined by the particle velocity and hardness. However, Pb can obtain sufficient contact with the metal substrate under very low velocity. Thus, the temperature has little effect on the bonding strength. The morphologies of the broken surfaces verify this point. It is clear that no deformation occurs on

the Q235 substrate. On the other hand, the Pb particles experience large deformation, which can be found in Figure 6 (the red arrow points to these typical locations). The three coatings are all very compact at the interface. There are almost no pores found on the surface. Iron is not found in the EDS, which means that no iron substrate was pulled from the substrate. From the substrate side, many Pb spots are left on the iron substrate.

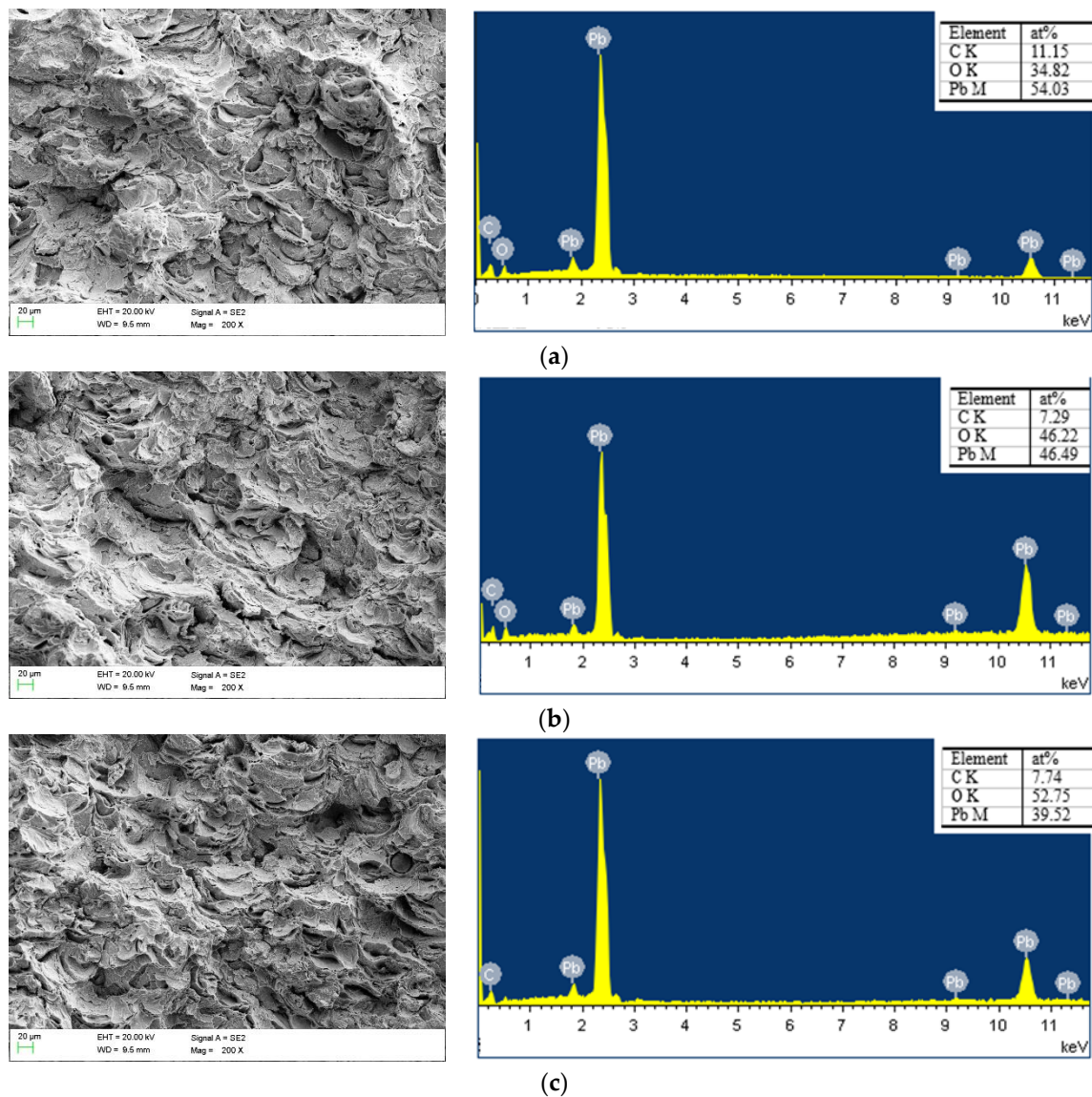


**Figure 6.** Micromorphology of cold sprayed Pb coatings on Q235 Steel after pull-off test (coating side): (a) 298 K, 1.6 MPa; (b) 348 K, 1.6 MPa; (c) 398 K, 1.6 MPa.

**Table 2.** Bonding strengths of cold sprayed Pb coatings under different spraying parameters (MPa).

Sample Numbers	Pb-1	Pb-2	Pb-3
Bonding strength	7.42	6.71	6.82
	6.66	7.75	6.52
	6.25	7.55	7.35
Average bonding strength	6.78 ± 0.59	7.34 ± 0.55	6.90 ± 0.42

### 3.3. Electrochemical Performance of Cold Sprayed Pb Coating

#### 3.3.1. Potentiodynamic Polarization Test

Figure 7 displays the potentiodynamic polarization curves of different electrodes in 0.5 M Na<sub>2</sub>SO<sub>4</sub> solution at a scan rate of 0.167 mV/s. There are three evident current peaks at the anodic area, each representing the corrosion of Pb, the formation of PbO<sub>2</sub>, and the evolution of oxygen, respectively. At the potential of −0.486 V, corrosion of Pb occurs and then the current density dramatically drops to about 1 μA/cm<sup>2</sup> (maintaining passivity current density). This means that when polarized to positive potential, the corrosion current remains small, which guarantees the long-term service life of the Pb electrode. At this stage, PbO<sub>2</sub> is formed on the surface which inhibits corrosion by passivation. As the potential drifts positively to 1.235 V, Pb ions or Pb is oxidized to PbO<sub>2</sub>. Then, the potential drifts positively to 1.522 V and oxygen evolution occurs. Because the corrosion current is much lower, the Pb electrode has a much longer life for electrolysis. There is little difference among the three kinds of sample, which indicates that although the oxygen content is different, it doesn't influence the electrochemical behavior much, since, as the potential becomes positive, the surface state will change to the same situation. The current density for each sample is about 1.2 μA/cm, which results in a very low corrosion rate.

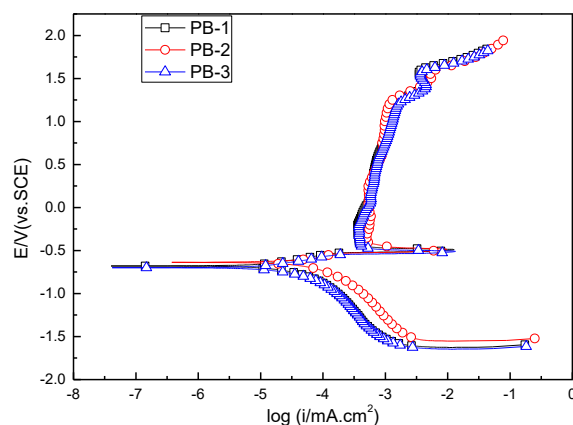


**Figure 7.** Potentiodynamic polarization curves of cold sprayed Pb coatings on Q235 Steel in saturated Na<sub>2</sub>SO<sub>4</sub> solution.

#### 3.3.2. Cyclic Voltammetry Behavior of PbO<sub>2</sub> Electrodes

The cyclic voltammetry curves are shown in Figure 8 for three different Pb coatings. It can be seen that the current peak location is similar to the polarization curves. Peak C in each graph stands for the hydrogen evolution (−1.5 V). Peak A is the oxidation of Pb to Pb<sup>2+</sup> (−0.4 V). Peak B is the reduction of Pb<sup>2+</sup> to Pb (−1.0 V). Peak D is the oxidation Pb<sup>2+</sup> to Pb<sup>4+</sup> (1.2 V). Peak E is the oxygen evolution (1.5 V). Apparently, the current peak height in each graph is different for different scanning rates. As the potential scanning rate increases, the current peak height increases, which means that the reactions of this system are all nonreversible to some extent. However, the reaction of Pb electrode is not completely nonreversible because a reduction peak exists for both the reaction of Pb to Pb<sup>2+</sup> and Pb<sup>2+</sup> to Pb<sup>4+</sup>. The dissolution of Pb is not similar to other metals, and most of the dissolved Pb remains on the electrode in the oxidized form. Then, while the potential drifts to negative, the reduction of oxidation occurs. For other metals, the metal enters into the solution and no reaction occurs when the potential is polarized to negative and no current peak can be observed. The solubility of Pb<sup>2+</sup> is limited. Most of the Pb<sup>2+</sup> exists in the form of Pb<sub>2</sub>SO<sub>4</sub>, and most of the Pb<sup>4+</sup> exists in the form of PbO<sub>2</sub>. It can be seen that Pb oxidation to Pb<sup>2+</sup> has two current peaks. The reduction of hydrogen and the oxidation of oxygen has only one peak and the oxygen and hydrogen in solution cannot support the reaction at the interface to produce a current peak. The oxygen evolution potential is about 1.525, 1.562,

and 1.523 V, respectively. This potential has little difference from titanium-based  $\text{PbO}_2$  electrodes [19]. There is little difference among the three samples.

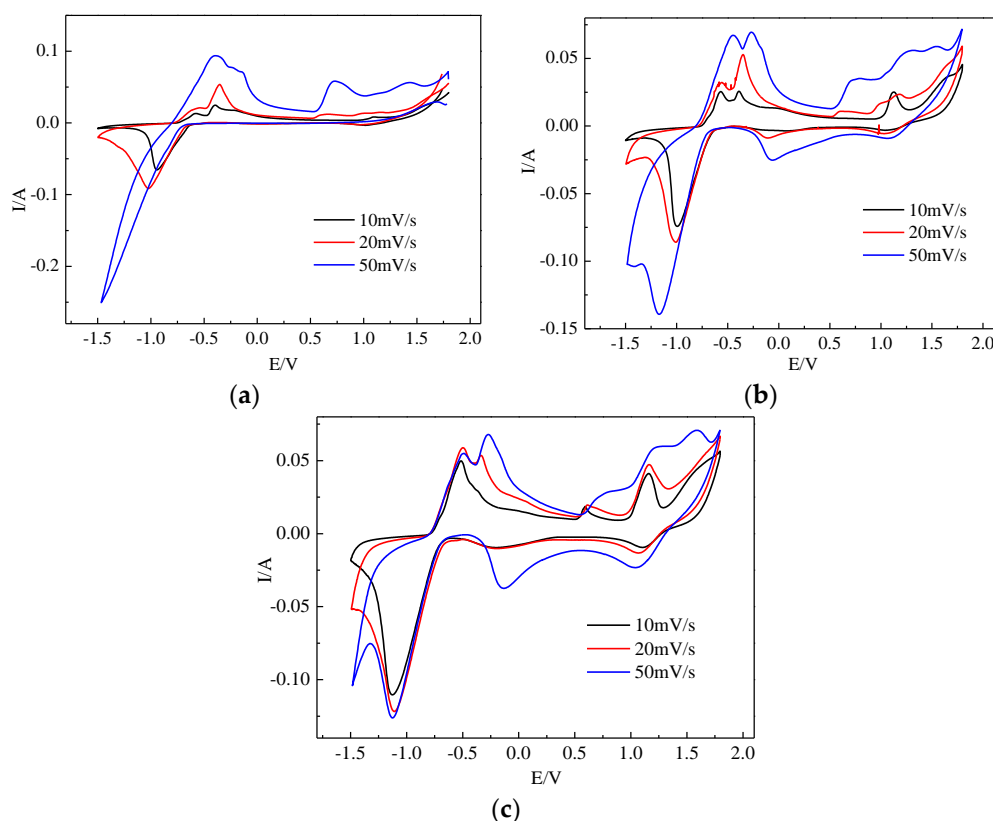


**Figure 8.** Evolution of LSV (linear sweep voltammetry) curves of cold sprayed Pb coatings on Q235 Steel in saturated  $\text{K}_2\text{SO}_4$  solution: (a) 298 K, 1.6 MPa; (b) 348 K, 1.6 MPa; (c) 398 K, 1.6 MPa.

### 3.3.3. Accelerated Electrolytic Life of $\text{PbO}_2$ Anode

Figure 9 shows the accelerated electrolytic life of a cold sprayed Pb anode in  $1 \text{ mol}\cdot\text{L}^{-1} \text{H}_2\text{SO}_4$  solution under the current density of  $1 \text{ A}/\text{cm}^2$ . It can be seen that both of the anodes have the same life cycle. The cell voltage of each sample is maintained at about 3.98 to 4.55 V. This is different from the cell voltage of titanium-based  $\text{PbO}_2$ , which has a voltage of about 6.2 V [20,21]. The cell voltage of Pb electrodes does not rise significantly during the whole electrolysis test. For titanium-based  $\text{PbO}_2$  anodes, the cell voltage rises abruptly mainly due to the passivation of titanium metal. The titanium oxide will increase the resistance of the electrolysis system. However, for Pb anodes, the Pb oxides are all conductive, and the Pb is oxidized to any of the oxides, but the resistance of the system will not increase. The weight loss of Pb electrodes under the current of  $1 \text{ A}/\text{cm}^2$  is listed in Table 3. The weight losses for the three kinds of Pb electrode are similar to each other. The Pb-3 samples has the lowest weight loss. There are two possible reasons leading to this difference. The Pb-3 samples were prepared under the highest temperature, thus their oxidation degree is the greatest. Then, during the electrolysis process, less Pb was oxidized. The second reason is that the corrosion rate on a rough surface is much higher than on a smooth one. There are some differences between the three kinds of sample. The spraying parameters can influence the particle boundary state, the boundary of deposited particles is more compact, and the corrosion rate is smaller. The coating with high spraying parameter has a more compact microstructure and a greater thickness [22,23]. However, Pb is different from other metals. Although it is very active in solution, it has a very low corrosion rate due to passivation. Pb is also a cathodic metal to Q235 steel, so it is important to avoid through-thickness pores. Previous

work [24,25] on WC-Co coated AA 7075-T6 also indicated that the high density of WC-Co coating guaranteed its anticorrosion performance.

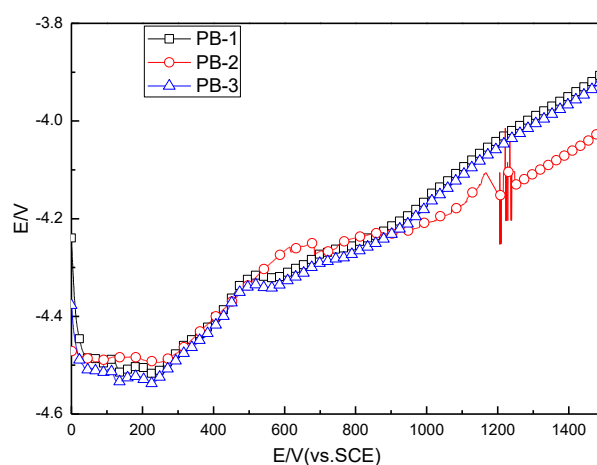


**Figure 9.** Variation of cell voltage with electrolysis time for Pb/Q235 Steel system in  $H_2SO_4$  solution.

**Table 3.** Weight losses of Pb samples under the current of  $1 A/cm^2$  ( $g \cdot dm^{-2} \cdot A^{-1} h^{-1}$ ).

Sample Numbers	Pb-1	Pb-2	Pb-3
Weight losses	5.115	5.013	4.995
	5.117	5.022	4.966
	5.125	5.021	4.976
Average weight loss	$5.119 \pm 0.005$	$5.019 \pm 0.005$	$4.979 \pm 0.015$

#### 4. Discussion

Compared to the thermal spraying method, cold spraying uses a much lower temperature, which is usually lower than 473 K. For any of the thermal spray methods, the spraying temperature is higher than 2000 K. However, the thermal spray methods still cannot achieve a full, dense coating because the melting particles in the spraying process are cooled down to a semi-melting state. Low velocity impaction makes the deformation of particles incomplete and leaves pores in the coating. The high temperature increases the oxidation degree. This worsens the impacting process because the increased oxide on the surface needs more energy to be deformed. The deformation rate decreases then increases the porosity further. For cold spraying methods, the oxidation is relatively low and high velocity particles can undergo complete deformation when impacting the substrate. The polarization curves show that the Pb coating has a very low passivation at a current of  $1 \mu A/cm^2$ , which means that under positive polarization the weight loss is very low, about  $0.34 \mu m/h$  by calculation. There is also no penetration phenomenon found in the polarization experiments. All experimental results and discussions indicate that cold sprayed Pb coating is a potential method for manufacturing Pb electrodes as an alternative to  $PbO_2$  electrodes.

#### 5. Conclusions

In the present work, the cold spraying method was used to deposit a smooth Pb coating on Q235 steel substrate for use as an anode. The physical properties were characterized by EDS, SEM, and other methods. The electrochemical performances were evaluated by potentiodynamic polarization curve, cyclic voltammetry, and accelerating electrolysis testing. Based on the above data and analysis the following conclusions can be drawn.

The coating has good physical performance, the porosity is less than 1%, and the bonding strength ranges from 5.25 to 7.75 MPa. The cross-sectional morphology suggests that no through-thickness pores exist in the coating.

Dynamic polarization curves of coated samples in sodium sulfate solution indicate that cold sprayed Pb coating is a good electrode for reduction of organic waste. Our results mean that cold spraying is capable of manufacturing electrode materials for electrochemical industries. The oxygen evolution potential is similar to the potential of titanium-based PbO<sub>2</sub> electrodes.

Cold sprayed Pb coatings have promising electrochemical performance and mechanical strength, and can be used for industrial applications in electro dialysis, electrolysis, and electrodeposition as an alternative to PbO<sub>2</sub> electrodes.

**Author Contributions:** Conceptualization, G.H. and W.F.; Methodology, G.H.; Validation, W.F., G.H. and Y.Z.; Formal Analysis, G.H.; Investigation, G.H.; Data Curation, W.F.; Writing—Original Draft Preparation, Y.Z.; Writing—Review and Editing, Y.Z. and G.H.

**Funding:** The project was supported by The State Key Laboratory for Marine Corrosion and Protection, Luoyang Ship Material Research Institute (No. JS1802).

**Acknowledgments:** The Pb powders was sieved properly by engineer Qiujiang Lan of Hebei Zhuhang Powder company.

**Conflicts of Interest:** The authors declare no conflict of interests.

## References

1. Li, Y.N.; Zhuang, X.Y.; Li, H.Y.; Ai, L.M.; Wang, Y.H.; Wang, Q.; Chen, H.Y.; Xia, J.X.; Xing, X. Fabrication and water treatment application of high efficient PbO<sub>2</sub> electrode. *Key Eng. Mater.* **2017**, *727*, 821–829. [[CrossRef](#)]
2. Hämeenoja, E.; Laitinen, T.; Sundholm, G. The formation of soluble Pb(IV) and Pb(II) species in the reactions of the PbSO<sub>4</sub>/PbO<sub>2</sub> electrode. *Electrochim. Acta* **1987**, *32*, 187–189. [[CrossRef](#)]
3. Hao, X.; Dan, S.; Qian, Z.; Honghui, Y.; Yan, W. Preparation and characterization of PbO<sub>2</sub> electrodes from electro-deposition solutions with different copper concentration. *RSC Adv.* **2014**, *4*, 25011. [[CrossRef](#)]
4. Ueda, M.; Watanabe, A.; Kameyama, T. Performance characteristics of a new type of lead dioxide coated titanium anode. *J. Appl. Electrochem.* **1995**, *25*, 817–822. [[CrossRef](#)]
5. Pavlov, D.; Monahov, B. Temperature dependence of the oxygen evolution reaction on the Pb/PbO<sub>2</sub> electrode. *J. Electrochem. Soc.* **1998**, *145*, 70–77. [[CrossRef](#)]
6. Hampson, N.A.; Jones, P.C.; Phillips, R.F. Electrochemical reactions at PbO<sub>2</sub> electrodes. Part IV. electrochemical. *Can. J. Chem.* **2011**, *47*, 2171–2179. [[CrossRef](#)]
7. Fengbang, S.; Buming, C.; Zhongcheng, G.; Siqi, D.; Yali, H. Preparation and characterization of β-PbO<sub>2</sub>-TiO<sub>2</sub>-Co<sub>3</sub>O<sub>4</sub> composite coating on stainless steel. *Chin. J. Appl. Chem.* **2012**, *29*, 691–696.
8. Velichenko, A.B.; Knysh, V.A.; Luk'yanenko, T.V.; Danilov, F.I.; Devilliers, D. PbO<sub>2</sub>-TiO<sub>2</sub> composite electrodes. *Prot. Met. Phys. Chem. Surf.* **2009**, *45*, 327–332. [[CrossRef](#)]
9. Zhou, X.Z.; Liu, S.Q.; Yu, H.X.; Xu, A.L.; Li, J.S.; Sun, X.Y.; Shen, J.Y.; Han, W.Q.; Wang, L.J. Electrochemical oxidation of pyrrole, pyrazole and tetrazole using a TiO<sub>2</sub> nanotubes based SnO<sub>2</sub>-Sb/3D highly ordered macro-porous PbO<sub>2</sub> electrode. *J. Electroanal. Chem.* **2018**, *826*, 181–190. [[CrossRef](#)]
10. Kumar, S.; Vidyasagar, V.; Jyothirmayi, A.; Joshi, S.V. Effect of heat treatment on mechanical properties and corrosion performance of cold-sprayed tantalum coatings. *J. Therm. Spray Technol.* **2016**, *25*, 745–756. [[CrossRef](#)]
11. Koivuluoto, H.; NiKki, J.; Vuoristo, P. Corrosion properties of cold-sprayed tantalum coatings. *J. Therm. Spray Technol.* **2009**, *18*, 75–82. [[CrossRef](#)]
12. Papyrin, A. Cold spray technology. *Adv. Mater. Process.* **2001**, *159*, 49–51.
13. Goldbaum, D.; Poirier, D.; Irissou, E.; Legoux, J.G.; Moreau, C. Review on cold spray process and technology US patents. In *Modern Cold Spray*; Springer International Publishing: Cham, Switzerland, 2015.
14. Hussain, T.; McCartney, D.G.; Shipway, P.H.; Zhang, D. Bonding mechanisms in cold spraying: The contributions of metallurgical and mechanical components. *J. Therm. Spray Technol.* **2009**, *18*, 364–379. [[CrossRef](#)]
15. Schmidt, T. Development of a generalized parameter window for cold spray deposition. *Acta Mater.* **2006**, *54*, 729–742. [[CrossRef](#)]

16. Koivuluoto, H.; Bolelli, G.; Lusvardi, L.; Casadei, F.; Vuoristo, P. Corrosion resistance of cold-sprayed Ta coatings in very aggressive conditions. *Surf. Coat. Technol.* **2010**, *205*, 1103–1107. [[CrossRef](#)]
17. *ASTM D4541-02 Standard Test Method for Pull-Off Strength of Coatings Using Portable Adhesion Testers*; ASTM International: West Conshohocken, PA, USA, 2010.
18. Grujicic, M.; Zhao, C.L.; Tong, C.; DeRosset, W.S.; Helfritsch, D. Analysis of the impact velocity of powder particles in the cold-gas dynamic-spray process. *Mater. Sci. Eng. A* **2004**, *368*, 222–230. [[CrossRef](#)]
19. Huang, R.; Fukanuma, H. Study of the influence of particle velocity on adhesive strength of cold spray deposits. *J. Thermal Spray Technol.* **2012**, *21*, 541–549. [[CrossRef](#)]
20. Dong, Y.J.; Lin, H.B.; Liu, X.B.; Ren, X.B.; Jiang, M. A cyclic voltammetric study of phenol on Ti/PbO<sub>2</sub> electrode in H<sub>2</sub>SO<sub>4</sub> solution. *Acta Chim. Sin.* **2007**, *65*, 2257–2260.
21. Tang, W.; Chen, Q.; Chen, Z.; Zhang, X.; Chai, W.; He, Z. Numerical simulation for effect of powder carrier gas on flow field and particle impact velocity in cold spraying. *J. Xi'an Jiaotong Univ.* **2012**, *46*, 82–86. (In Chinese)
22. Silva, F.S.D.; Cinca, N.; Dosta, S.; Cano, I.G.; Couto, M.; Guilemany, J.M.; Benedetti, A.V. Corrosion behavior of WC-Co coatings deposited by cold gas spray onto AA 7075-T6. *Corros. Sci.* **2018**, *136*, 231–243. [[CrossRef](#)]
23. Almangour, B.; Mongrain, R.; Irissou, E.; Yue, S. Improving the strength and corrosion resistance of 316L stainless steel for biomedical applications using cold spray. *Surf. Coat. Technol.* **2013**, *216*, 297–307. [[CrossRef](#)]
24. Couto, M.; Dosta, S.; Guilemany, J.M. Comparison of the mechanical and electrochemical properties of WC-17 and 12Co coatings onto Al7075-T6 obtained by high velocity oxy-fuel and cold gas spraying. *Surf. Coat. Technol.* **2015**, *268*, 180–189. [[CrossRef](#)]
25. Kumar, S.; Jyothirmayi, A.; Wasekar, N.; Joshi, S.V. Influence of annealing on mechanical and electrochemical properties of cold sprayed niobium coatings. *Surf. Coat. Technol.* **2016**, *296*, 124–135. [[CrossRef](#)]



© 2019 by the authors. Licensee MDPI, Basel, Switzerland. This article is an open access article distributed under the terms and conditions of the Creative Commons Attribution (CC BY) license (<http://creativecommons.org/licenses/by/4.0/>).